

TCDSG: An End-to-End Approach for Action Tracklet Generation

Raphael Ruschel
UC Santa Barbara
raphael1251@ucsb.edu

Md Awsafur Rahman
UC Santa Barbara
awsaf@ucsb.edu

Hardik Prajapati
UC Santa Barbara
hprajapati@ucsb.edu

Suya You
ARL West
suya.you.civ@army.mil

B. S. Manjunath
UC Santa Barbara
manj@ucsb.edu

Abstract

*Comprehensive video scene understanding centers on modeling the temporal evolution of object interactions across frames. Methods that operate framewise often fragment tracklets and break subject–object linkages, limiting long-term activity analysis. We present **Temporally Consistent Dynamic Scene Graphs (TCDSG)**, a unified end-to-end framework that jointly performs detection, tracking, and interaction linking across video sequences. TCDSG is driven by two key ideas. First, a temporal bipartite matching strategy maintains stable query assignments across frames, substantially reducing tracklet fragmentation without post-processing. Second, adaptive decoder queries augmented with inter-frame feedback inject temporal context directly into decoding, yielding more stable and accurate predictions. As a result, TCDSG retains competitive single-frame accuracy while substantially boosting temporal consistency; for example, tR@50 improves from 18.6% to 39.1% on Action Genome. We evaluate on Action Genome, OpenPVSG, and MEVA, demonstrating consistent gains in spatio-temporal interaction tracking. To support rigorous long-range evaluation, we also re-annotate a subset of MEVA with persistent cross-frame object IDs, addressing inconsistencies in the original annotations. The simplicity, robustness, and temporal fidelity of TCDSG make it well suited for continuous video analytics in surveillance, autonomous systems, and human–computer interaction.*

1. Introduction

Understanding actions in video underpins applications in large-scale monitoring [31], human–computer interaction [5, 38], and autonomous systems [1]. Scene graphs provide a structured way to encode object relationships, but most work remains *frame-centric*: associations are recomputed independently per frame, so subject–object links

rarely persist over time. This gap limits long-range interaction tracking and motivates temporally consistent scene-graph models.

Figure 1 presents an example of an input video sequence and the corresponding desired output that includes a triplet $\langle \text{subject}, \text{object}, \text{relationship} \rangle$, along with bounding boxes and timestamps to denote the activity.

Recent advances in action detection and scene graph generation have made impressive progress in modeling spatial relationships within frames [17, 18, 51]. While some methods address challenges like compositionality [19] and dataset biases [36], they approach video understanding as essentially a series of independent frame analyses. Current temporal aggregation strategies typically rely on post-processing to connect frame-level predictions [26, 59], which introduces several critical limitations:

1. Post-processing methods cannot leverage inter-frame information during the detection stage itself
2. Object identities may swap in crowded scenes
3. Heuristic linking requires fine-tuning and reduces generalization across datasets

This fundamental disconnect between detection and tracking creates fragmented action tracklets that fail to capture the continuous nature of real-world activities. What’s needed is not merely better post-processing, but an approach that inherently maintains temporal consistency throughout the detection process. To tackle this challenge, we introduce TCDSG: Temporally Consistent Dynamic Scene Graphs, an innovative end-to-end pipeline designed to generate seamless action tracklets across entire video sequences. By integrating our approach into existing architectures with minimal modifications, we achieve substantial gains in temporal consistency for both object tracking and relationship prediction, enabling more robust and continuous video analysis.

We evaluate TCDSG on three benchmark datasets: Action Genome, OpenPVSG, and MEVA, demonstrating state-

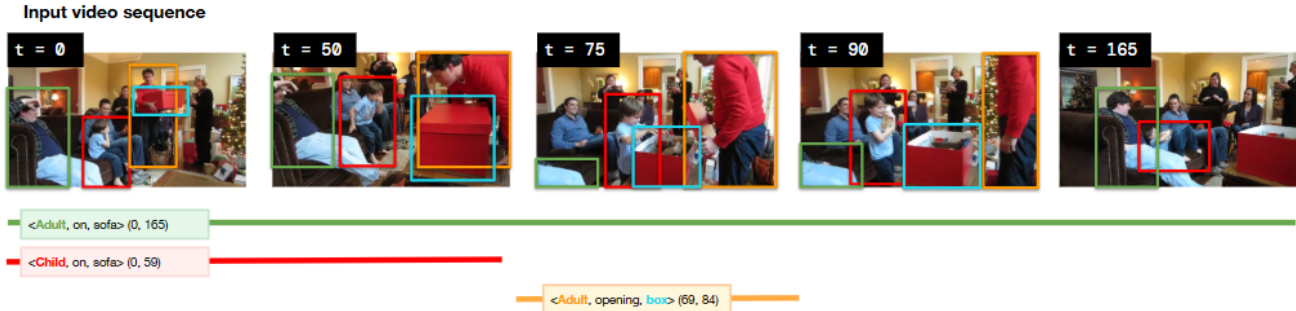


Figure 1. An example of the desired output for a video sequence. At the top, we show a few selected frames and their corresponding timestamp, and at the bottom, distinct action tracklets. Each interaction displays a triplet \langle subject, object, relationship \rangle alongside the associated bounding box (color-coded) and timestamps. For clarity, only select interactions are annotated.

of-the-art performance in tracklet consistency and competitive framewise prediction. Additionally, we provide a new set of annotations for a subset of the MEVA dataset, where we uniquely identify each object, further validating our approach. Our main contributions include:

- **Sequence-Level Objective for Temporally Coherent Assignment:** We propose a paradigm shift by redefining the matching objective to operate across time. Instead of optimizing over per-frame entities, we optimize over evolving data trajectories, persistently binding triplets to decoder queries and penalizing identity switching. This sequence-aware formulation is implemented as a lightweight extension of Hungarian matching and enables temporally aligned predictions directly from training.
- **Temporally Conditioned Decoder Queries:** We design decoder queries that evolve contextually with the video by integrating outputs from previous frames through a cross-attentional feedback loop. This equips the model with memory, temporal context, and continuity, reducing improving prediction stability over time.
- **Enhanced MEVA annotations:** We extend a subset of the MEVA dataset with unique, persistent object IDs, resolving the issue of inconsistent or missing annotations in high-traffic scenes. Although this subset is not the entire dataset, these refined labels enables advanced tracklet generation over longer videos and set a foundation for future work in large-scale dynamic scene understanding.

2. Related works

2.1. Scene Graph Generation

Scene graph generation (SGG) involves creating a graph-like structure where nodes represent objects in a scene and edges represent relationships between these objects, such as actions (e.g., *holding*, *sitting*, *walking*) and spatial relationships (e.g., *close*, *to the right of*, *above*). Originally

introduced for image retrieval [23], SGG has since become foundational for applications in monitoring, interactive systems, and human-computer interfaces. Early work focused on *static SGG*, generating scene graphs for single images [4, 7, 8, 34, 43, 46, 48, 54, 55].

Considerable effort has been devoted to tackling challenges in SGG, such as compositionality and dataset biases. For instance, [19] examines compositional SGG to improve recall for unseen triplets formed from known objects and relationships, and also discusses limitations of the two-stage SGG pipeline used in [14, 28, 32, 48, 49, 53]. Additionally, addressing biases from long-tailed distributions is an ongoing focus [33, 36].

Recent advancements have expanded SGG to dynamic scenes [9, 22, 30, 47, 61], aiming to generate scene graphs across video sequences by harnessing temporal context. Unlike static SGG, dynamic SGG captures time-dependent actions (e.g., *picking up* vs. *putting down*), which require an understanding of temporal dependencies. Temporal consistency becomes essential here, as it supports the accurate interpretation of activities that evolve over time.

An important development in this field is Panoptic Video Scene-Graph Generation (PVSG) [59], which introduces action tracklets for temporal activity understanding. This work also proposes the use of panoptic segmentation masks instead of bounding boxes, achieving pixel-level localization for subjects and objects. However, this approach depends on post-processing to aggregate results over time, limiting its utility for applications that require temporal consistency in an end-to-end framework.

2.2. Tracking

Object tracking in computer vision focuses on detecting and following objects throughout video sequences to capture their trajectories, a capability essential for applications like autonomous driving, surveillance, action recognition, and augmented reality. Traditional approaches, including

Kalman filters [57] and mean-shift algorithms [63], have evolved with deep learning to form sophisticated multi-object tracking (MOT) systems based on CNNs and transformers.

Many approaches [2, 25, 40, 58] address tracking as a combination of appearance and motion cues. However, they rely on post-processing to merge appearance and motion, which often results in suboptimal temporal dependency modeling across frames, limiting its effectiveness for tracking continuous actions. TransTrack [45], for example, uses a transformer-based approach for bounding box generation but requires post-processing for IoU-based matching.

While TransTrack leverages transformers for detection, its reliance on post-processing for association contrasts with truly end-to-end approaches like MOTR [60] and TrackFormer [35] which integrate detection and association directly within their transformer architectures. TrackFormer extend DETR [3] by treating tracking as a *tracking-by-attention* task, using attention maps for both tracking and detection. MOTR’s tracklet-aware label assignment scheme manages new and stale tracklets dynamically through variable-length track queries.

Despite significant progress, existing methods fall short of unifying activity recognition and object tracking within a fully end-to-end framework. Current approaches treat these tasks in isolation, missing the opportunity to leverage their synergy. TCDSG precisely addresses this critical void by simultaneously capturing complex interactions and object trajectories, which is crucial for advancing applications like trajectory analysis, seamless human-computer interaction, and real-time monitoring in dynamic environments.

3. Methodology

In this section, we present our Temporally Consistent Dynamic Scene Graphs (TCDSG) framework for generating coherent action tracklets from video sequences. We first formulate the problem and then describe the architecture, temporal bipartite matching, loss functions, and evaluation metrics. We conclude with a pseudocode outline summarizing the key components of our approach.

3.1. Problem Formulation

Given a video sequence $V = \{I_1, I_2, \dots, I_T\}$ of T frames, the goal is to predict a set of action tracklets $\mathcal{AT} = \{at_1, at_2, \dots, at_M\}$, where M is the number of distinct actions occurring in V . Each action tracklet at_i is represented as:

$$at_i = \langle s_i, o_i, r_{s,o}, \mathcal{B}_s, \mathcal{B}_o, t_{start}, t_{end} \rangle$$

where:

- s_i and o_i denote the subject and object class labels,
- $r_{s,o}$ is the relationship predicate between subject and object,

- \mathcal{B}_s and \mathcal{B}_o are sequences of bounding boxes for subject and object from t_{start} to t_{end} ,
- t_{start} and t_{end} are the start and end frame indices of the tracklet.

Our objective is to generate temporally consistent predictions that maintain coherent identities and relations across the entire video duration.

3.2. Network Architecture

Our architecture builds upon transformer-based detection frameworks such as Deformable DETR [64] and DDS [19], with key modifications to model temporal consistency explicitly. A diagram of our full network is shown in Figure 2.

Backbone and Feature Extraction: We employ a ResNet-50 backbone [16] to extract multi-scale feature maps shared across two parallel branches:

- **Object branch:** predicts object classes and bounding boxes, we consider every unique class in the dataset as possible *subjects* and *objects*.
- **Relationship branch:** predicts predicates between subject-object pairs.

3.3. Temporally Conditioned Queries (TCQ)

DETR-style transformers rely on static learnable queries, which lack temporal awareness. We introduce *temporally conditioned decoder queries* that evolve by incorporating outputs from prior frames. Specifically, the input queries at frame t are a function of both learnable embeddings and the output embeddings from frame $t - 1$, enabling the decoder to adaptively refine its predictions with temporal context. Previous approaches that incorporates feedback from the previous stages, such as [19], typically just feed the output from the previous frame as input to the current one, however, this presents a shortcoming since the the output from frame $t - 1$ is detached from the computation graph, so no gradients will flow through that path during processing of frame t . Despite providing significant improvements, we expand on this approach by adding a simple LSTM layer connecting $t - 1$ to t , ensuring that we maintain an updated state after each frame gets processed.

Formally, the query embeddings \mathbf{Q}_t at frame t are computed as shown in Equation 1:

$$\mathbf{Q}_t = f(\mathbf{Q}_{learn}, \text{LSTM}(\mathbf{D}_{t-1})) \quad (1)$$

where \mathbf{Q}_{learn} are learned query embeddings, $\text{LSTM}(\mathbf{D}_{t-1})$ is temporal summary of previous decoder outputs, and $f(a, b)$ denotes the cross-attention operation using a as input queries and b as query and value. This design imparts:

- **Memory:** retaining information from prior predictions
- **Context:** leveraging temporal dependencies beyond spatial features

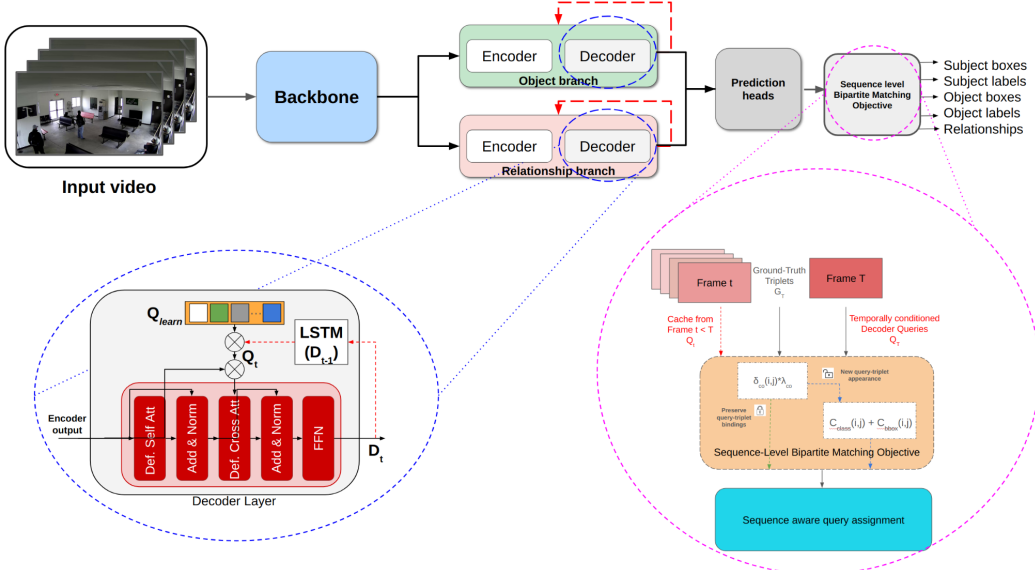


Figure 2. Overview of the TCDSG architecture. A shared CNN backbone extracts features that are fed into two parallel transformer decoder branches for subjects, objects, and relationships. The architecture integrates two key innovations: **(1) Temporally Conditioned Decoder Queries** (lower left zoomed-in block) that incorporate LSTM-based feedback and cross-attentional context from prior frames, and **(2) the Sequence-Level Bipartite Matching Objective** (lower right zoomed-in block), which modifies Hungarian matching with a temporal penalty to preserve query-triplet identities across frames. Feedback connections propagate temporal information, enabling end-to-end temporally coherent predictions.

- **Continuity:** ensuring that predictions evolve smoothly with the video’s narrative.

In Figure 2 we show the architecture of our decoders in more details, illustrating this feedback process in detail.

3.4. Sequence-Level Bipartite Matching Objective (SLBM)

A core contribution of our method is a *sequence-level bipartite matching objective* that optimizes over evolving data trajectories, thus preserving identity across time: once a ground-truth triplet is assigned to a decoder query, we strongly bias subsequent frames to keep that association. This simple change—a lightweight extension to standard Hungarian matching—greatly reduces tracklet fragmentation and yields temporally stable triplet predictions without post-processing. This mechanism is highlighted in the SLBM module of Figure 2

Standard Hungarian Matching: Our architecture follows the DETR formulation [3], in which each frame produces N_q set-prediction slots ($N_q > N_{\text{obj}}$) and a one-to-one assignment between predictions and ground-truth objects is computed via Hungarian matching during training. In its vanilla form, standard Hungarian matching minimizes per-frame assignment costs:

$$C_t(i, j) = C_{\text{class}}(i, j) + C_{\text{bbox}}(i, j) \quad (2)$$

While effective for static scenes, this formulation fails to

preserve temporal continuity. As a result, a ground-truth instance (or subject–object–relation triplet) assigned to query q at frame I_t may be reassigned to any other query $q' \in \{1, \dots, N_q\}$ at frame $I_{t+\Delta}$ with no penalty, requiring additional post-processing [42]. Over a sequence, these unconstrained framewise permutations cause the *same* triplet to hop across queries, degrading temporal linkage and fragmenting downstream tracklets.

Temporal Consistency Enforcement: To impose cross-frame identity, we cache each ground-truth triplet $\langle s, o, r_{s,o} \rangle$ the first time it appears and bind it to the decoder query to which it was matched. For all subsequent frames t , the Hungarian cost matrix is modified: any assignment that would re-map this previously locked triplet to a different query receives a large penalty λ_{co} . This simple cache-and-penalize extension to standard (per-frame) Hungarian matching [3, 42] sharply reduces tracklet fragmentation by preserving stable query→triplet identities across time. Because the constraint is injected during training, inference inherits temporally aligned query indices, allowing tracklets to be formed by straightforwardly grouping per-frame predictions by query.

Formally, for prediction i and ground truth j at frame t , the cost matrix C_t is as defined in 3:

$$C_t(i, j) = C_{\text{class}}(i, j) + C_{\text{bbox}}(i, j) + \delta_{co}(i, j) \cdot \lambda_{co} \quad (3)$$

Where $C_{\text{class}}(i, j)$ is the classification cost between

query i and ground-truth label j , similarly, $C_{box}(i, j)$ is the cost to match bounding box i to the j th ground-truth box. Lastly $\delta_{co}(i, j)$ is 1 if assignment conflicts with prior frames, and λ_{co} is a positive, large scalar. A pseudocode of the forward pass of our network during training is shown in Algorithm 1.

Algorithm 1 TCDSG forward pass

```

Input: Video frames  $\{I_1, \dots, I_T\}$ , learnable queries
 $\mathbf{Q}_{learn}$ 
Initialize hashmap  $\mathcal{H} \leftarrow \emptyset$  to store triplet-query assignments
for  $t = 1$  to  $T$  do
    Extract features  $\mathbf{F}_t$  from  $I_t$  via backbone
    if  $t = 1$  then
        Set query embeddings  $\mathbf{Q}_t \leftarrow \mathbf{Q}_{learn}$ 
    else
        Obtain previous decoder outputs  $\mathbf{D}_{t-1}$ 
        Update queries  $\mathbf{Q}_t$  as in Eq. 1
    end if
    Decode predictions  $\mathcal{P}_t$  from  $\mathbf{F}_t$  and  $\mathbf{Q}_t$ 
    Compute cost matrix  $C_t$ 
    for all triplets in  $\mathcal{H}$  do
        Add large penalty to corresponding entries in  $C_t$ 
    end for
    Perform Hungarian matching on  $C_t$ 
    for all  $(p_i, g_j) \in M_t$  do
        if  $g_j$  not in  $\mathcal{H}$  then
            Lock assignment:  $\mathcal{H}[g_j] \leftarrow p_i$ 
        end if
    end for
    Compute losses and update model parameters
end for

```

3.5. Loss Functions

Our total loss \mathcal{L} combines several terms balancing spatial accuracy, semantic consistency, and temporal stability, and is defined in Eq. 4:

$$\mathcal{L} = \lambda_{spat} \mathcal{L}_{spat} + \lambda_{const} \mathcal{L}_{const} + \lambda_{ref} \mathcal{L}_{ref} + \lambda_{label} \mathcal{L}_{label} \quad (4)$$

- **Spatial loss** \mathcal{L}_{spat} : combines generalized IoU and L_1 regression of the bounding box normalized coordinates.
- **Label Loss** \mathcal{L}_{label} : Cross-entropy for class labels, and focal loss for predicates as in prior work [3].
- **Consistency loss** \mathcal{L}_{const} : encourages feature embeddings of the same class across frames to be similar, improving temporal feature stability.
- **Reference point loss** \mathcal{L}_{ref} : The Reference point loss guides the initial reference points for deformable attention, typically towards object centers, to stabilize early-

frame predictions when dynamic query feedback from previous frames is not yet available (t=1)

3.6. Evaluation Metrics

We adopt temporal Recall@K ($tR@K$) to measure tracklet consistency. Unlike frame-level Recall@K, $tR@K$ requires predictions to have both spatial overlap (IoU ≥ 0.5) and sufficient temporal Intersection over Union with ground truth. This metric better reflects performance on continuous action understanding.

4. Datasets

To train and evaluate our method, we utilized three datasets that provide bounding box annotations for subjects and objects, along with their inter-relationships. Each dataset was adapted to ensure consistent object identifiers, crucial for robust tracking.

4.1. Action Genome (AG)

Action Genome (AG) [21] extends the Charades dataset [44] with frame-level scene graph annotations. AG provides bounding box and relationship annotations for 36 object and 25 relationship classes. However, subjects are exclusively labeled as "person," and unique identifiers for tracking are not provided.

To enable tracking, we implemented a pseudo-labeling strategy to assign consistent object identifiers across frames based on bounding box overlap. While this approach may introduce noise if distinct objects of the same class frequently enter and exit the scene, our manual verification indicated that such instances typically involved the same object re-entering, validating our methodology's applicability.

4.2. OpenPVSG

The OpenPVSG dataset [59] was developed for Panoptic Video Scene Graph Generation (PVSG), which extends traditional scene graph generation with pixel-level segmentation masks. Comprising 400 videos (averaging 76.5 seconds at 5 FPS) sourced from VidOR [41], EpicKitchen [11], and Ego4D [15], OpenPVSG offers diverse indoor and outdoor scenes captured by both moving and static cameras. Unlike AG, OpenPVSG includes various subject types beyond "person" and provides unique object identifiers per video sequence, making it inherently suitable for tracking tasks.

OpenPVSG features 157 object classes (e.g., animals, furniture, food) and 57 relationship classes. For compatibility with our methodology, we converted the provided segmentation masks into bounding boxes by extracting the minimum and maximum coordinates.

Method	SGDet - With constraint					
	mR@20	mR@50	R@20	R@50	tR@20	tR@50
iSGG [24]	19.7	22.9	29.2	35.3	-	-
STTran-TPI [52]	20.2	21.8	29.1	34.6	-	-
APT [27]	-	-	29.1	38.3	-	-
TEMPURA [36]	22.6	23.7	33.4	34.9	-	-
VsCGG [33]	-	24.2	35.8	38.2	-	-
TD2-Net (p) [30]	-	23	28.7	37.1	-	-
DSG-DETR [13]	-	-	34.8	36.1	-	-
OED [50]	-	-	40.9	48.9	-	-
DDS [19]	29.1	32.2	42.0	47.3	13.5	18.6
TPT [62]	-	-	37.3	49.2	-	-
TCDSG* (Ours)	36.1	46.8	47.9	58.4	14.4	27.1
TCDSG (Ours)	27.8	38.9	41.6	52.5	17.5	39.1

Table 1. Comparisons on the Action Genome dataset under the SGDet (with constraint) protocol. While our method (**TCDSG**) yields competitive $R@k$, it exhibits substantially higher ($tR@k$), indicating its robust ability to capture relationships across longer sequences. For instance, $tR@50$ improves from 18.6 to 39.1 in certain settings, highlighting TCDSG’s effectiveness in generating coherent action tracklets over time. **TCDSG*** refers to our method when we remove the Temporal Hungarian Matching during training, showing the tradeoff between frame-level and temporal-based recall.

4.3. MEVA

The MEVA dataset [10] is a large-scale collection for activity detection in multi-camera environments. It comprises over 9300 hours of untrimmed video footage. Our study utilized 144 hours of annotated data covering 37 activity types, with corresponding bounding boxes for each instance. This data was collected from approximately 100 actors performing scripted scenarios over three weeks at an access-controlled venue, captured by 38 cameras configured for typical surveillance setups.

Despite its scale, MEVA presents several annotation challenges:

- Some relationships lack a standard `<subject, object, relationship>` triplet format (e.g., “vehicle reverses” without an explicit object).
- Certain relationship classes embed objects within their labels (e.g., “person opens facility door”), but the corresponding objects may lack bounding box annotations.
- Intended unique track IDs often result in multiple IDs for the same individual within a single video sequence, compromising tracking reliability.

We therefore re-annotated a subset of MEVA with unique, cross-frame object IDs, enabling consistent multi-frame evaluation under our $R@K$ / $tR@K$ metrics. Our additional annotations for MEVA include 141 training videos ($\approx 400k$ frames across 16 cameras) and 47 test videos ($\approx 23k$ frames across 12 cameras, 3 of which were unseen during training). We focused on re-annotating the busiest regions of the dataset, such as the bus station, subway station, and the regions surrounding them.

4.4. Implementation Details

We use a ResNet-50 [16] backbone and train with AdamW [20] using BLoad [39] for efficient, distributed learning on variable-length videos.

Each branch uses a 6-layer encoder-decoder stack with $N_q=100$ 256-d queries. We initialize from DETR [3] weights pre-trained on COCO [29] and train for 20 epochs on $8 \times$ NVIDIA A100 GPUs, selecting the best checkpoint by validation metrics. The full model has 59M parameters and runs at ~ 20 fps using < 2 GB GPU memory at inference (no optimizations).

Inference & Tracklet Construction: During inference, TCDSG directly outputs coherent tracklets without post-hoc linking, no additional IoU linking, or ReID post-processing is required. Thanks to our temporal matching (Sec. 3.4), predictions maintain consistent query-triplet associations and are grouped by query index. For each frame we compute a joint confidence score per prediction, rank, and retain the top- k entries (consistent with $\text{Recall}@k$ evaluation). Tracklets are formed by concatenating consecutive frames whose predictions share the same query index and triplet label.

This native mapping yields tracklets that are temporally trimmed and identity-stable: a given query index corresponds to a single evolving $\langle s, o, r_{s,o} \rangle$ interaction for the duration of its visibility. If a previously active query drops from the top- k set or changes its predicted triplet, we close the current tracklet and (if re-emitted) initialize a new one, allowing graceful handling of occlusion, interaction changes, or confidence decay. Integrating detection,

relationship prediction, and temporal linking within one transformer-based pipeline is a key differentiator of TCDSG compared with methods that must post-hoc stitch per-frame scene graphs into action tracklets.

5. Results

5.1. Performance evaluation

We evaluate TCDSG on Action Genome against state-of-the-art scene-graph / HOI baselines. Table 1 aggregates reported results; metrics absent from original papers (e.g., tR@K) are shown as “–”. Figure 3 illustrates a representative qualitative comparison, highlighting the improved temporal coherence of our predictions. Additional qualitative results are included in the supplementary material.

Despite incomplete metric coverage across baselines, TCDSG delivers competitive single-frame Recall@K and substantially higher temporal scores. As shown in Table 1, it achieves the strongest tR@K, demonstrating stable subject–object relationship tracking over extended sequences. These gains follow from our temporally aware design—temporal bipartite matching and inter-frame feedback—which curbs query permutation and tracklet fragmentation common to framewise pipelines. Such long-horizon stability is critical for continuous video analytics in surveillance, monitoring, and activity understanding.

Although we evaluate OpenPVSG in *bounding-box mode* (converting its panoptic masks), it remains markedly more challenging than AG: clips are longer, object and predicate vocabularies are larger, and subjects span many categories (AG: subject always person), adding an additional label dimension to the matching problem. Accordingly, absolute recall values in Table 2 are lower than on AG. Even so, TCDSG yields improved temporal recall, underscoring its robustness under greater semantic and temporal variability.

Method	R@20	R@50	tR@20	tR@50
IPS + T [6, 56]	-	-	3.88	5.66
VPS [6, 26]	-	-	0.42	0.73
MACL [37]	-	-	4.5	6.0
TCDSG*	27.5	32.3	10.2	14.2

Table 2. Results on OpenPVSG dataset. For IPS+T and VPS results, we extracted the numbers from [59]. On our results, * denotes using bounding boxes as object location grounding.

MEVA Evaluation: MEVA poses additional challenges: most prior work (e.g., [12]) reports $P_{miss} @ X_{tfa}$ rather than Recall@K. In addition, we operate on the newly curated subset and with different metrics, direct comparison to prior MEVA reports is not meaningful.

MEVA’s long clips (up to ~ 5 min) provide a rigorous

stress test for temporal stability. We observed large gaps between framewise and temporal recall, motivating an analysis of *temporal sampling density*. In Table 3 we evaluate multiple subsampling factors (keeping every f^{th} frame). R@K remains stable, but tR@K improves markedly as f increases, suggesting that long unbroken sequences expose transient query switches that fragment tracklets; sparser sampling reduces these opportunities. Going forward, we plan to incorporate short-term multi-hypothesis or temporally smoothed assignment strategies to further suppress such transient switches in long-form video.

Subsample Factor	R@20	R@50	tR@20	tR@50
1	62.1	67.9	6.7	7.8
5	62.1	67.9	9.9	12.4
10	62	67.7	10.9	17
20	61.9	67.6	17.6	31.2

Table 3. Results on MEVA dataset with different subsampling factors on our proposed test set

6. Ablation Studies

We ablate TCDSG components on Action Genome (default dataset unless noted). Table 4 reports incremental additions to the baseline and their impact on frame-level Recall@K (R@K) and temporal Recall@K (tR@K).

Method	R@20	R@50	tR@20	tR@50
(1) Baseline	36.7	44.4	10.2	16.0
(2) SLBM	34.3	42.0	13.1	25.4
(3) TCQ	39.8	46.9	11.0	16.2
(4) Cos similarity + (2) + (3)	38	47.8	15.5	30.2
(5) \mathcal{L}_{ref} + (4)	39.7	51.0	16.5	35.6
(6) LSTM + (5)	41.6	52.5	17.5	39.1
(7) (6) – (2)	47.9	58.4	14.4	27.1

Table 4. Performance comparison of our baseline model and the effect of each proposed component on R@k and tR@k at different k values on the Action Genome dataset.

Baseline (No Temporal Locking): When run without temporal consistency enforcement, our network delivers competitive state-of-the-art frame-level Recall@K (R@K) on Action Genome, underscoring the strength of the underlying transformer architecture and adaptive query design for single-frame scene graph generation.

Adding Temporal Consistency: Introducing temporal bipartite matching—which preserves query identity across frames—can slightly reduce per-frame R@K. This is an intentional trade-off: once a query is “claimed” by a triplet, we discourage reassignments that might improve instantaneous detection at the cost of long-range coherence.

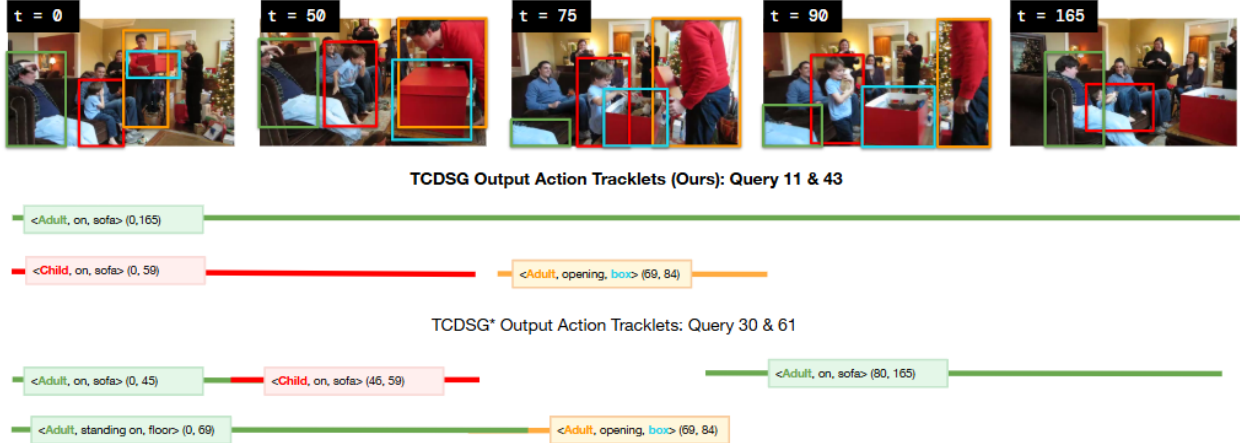


Figure 3. Comparative visualization of action tracklet continuity between TCDSG (our method) and TCDSG*, which represents our module without the proposed temporal matching. While TCDSG* produces fragmented tracklets with the same query producing different triplets, TCDSG maintains consistent query assignment throughout the video sequence. This persistent identity mapping enables continuous tracking of interactions over extended durations. For clarity, only boxes from TCDSG are plotted

The benefit of enforcing identity persistence is clear in temporal metrics. As shown in Table 1, TCDSG increases tR@50 from 18.6% (DDS) to 39.1% (+110% rel.), demonstrating substantially more stable subject–object relationship tracking over time. These results validate our end-to-end, temporally grounded formulation as a practical route to robust action tracklet generation.

Integrating cosine similarity significantly boosts temporal recall by enforcing consistency in feature representations across consecutive frames. This aligns with the understanding that features for recurring objects or interactions should remain stable throughout a video, given the inherently smooth temporal transitions.

The \mathcal{L}_{ref} is crucial for guiding the initial reference points of the deformable attention mechanism. This is especially beneficial in the early frames of a video sequence, where the model lacks sufficient temporal context, and the dynamic queries haven't yet accumulated enough information to effectively guide the model.

Lastly, incorporating an LSTM layer into the feedback loop serves to compute an internal state representation of the previous frame. The LSTM's inherent update and forget gates allow the network to selectively retain only the most informative data from previous queries, thereby refining temporal context and improving overall prediction stability.

7. Conclusion & Future Works

In this paper, we introduced TCDSG, an end-to-end pipeline designed to generate temporally consistent scene graphs,

enabling the creation of robust action tracklets that are applicable to various downstream tasks in video-based analytics and surveillance. Our approach introduces two key paradigm shifts for video scene understanding: a sequence-level objective for trajectory-aware query assignment, and temporally conditioned decoder queries that evolve dynamically with the scene. Together, these contributions enable robust action tracklet generation without post-processing, achieving strong temporal consistency across diverse datasets. Through evaluations on three benchmark datasets, TCDSG achieved state-of-the-art results in tracklet predictions while maintaining competitive performance on single-frame predictions.

Additionally, leveraging the rich MEVA dataset, we plan to explore Re-identification (ReID) capabilities across distinct cameras by having an additional ReID block on the network that access a centralized memory bank that contains shared information from all cameras. By focusing on cross-camera ReID, we can extend TCDSG's capabilities to track individuals across multiple camera views, a feature highly valuable in multi-camera surveillance setups. This enhancement has the potential to enable robust tracking across complex environments, supporting continuous monitoring in large-scale applications.

References

[1] Yuhao Bai, Baohua Zhang, Naimin Xu, Jun Zhou, Jiayou Shi, and Zhihua Diao. Vision-based navigation and guidance for agricultural autonomous vehicles and robots: A review. *Computers and Electronics in Agriculture*, 205:107584, 2023. 1

[2] Alex Bewley, Zongyuan Ge, Lionel Ott, Fabio Ramos, and Ben Upcroft. Simple online and realtime tracking. In *2016 IEEE international conference on image processing (ICIP)*, pages 3464–3468. IEEE, 2016. 3

[3] Nicolas Carion, Francisco Massa, Gabriel Synnaeve, Nicolas Usunier, Alexander Kirillov, and Sergey Zagoruyko. End-to-end object detection with transformers. In *European conference on computer vision*, pages 213–229. Springer, 2020. 3, 4, 5, 6

[4] Long Chen, Hanwang Zhang, Jun Xiao, Xiangnan He, Shiliang Pu, and Shih-Fu Chang. Counterfactual critic multi-agent training for scene graph generation. In *Proceedings of the IEEE/CVF International Conference on Computer Vision*, pages 4613–4623, 2019. 2

[5] Yanan Chen, Ang Li, Dan Wu, and Liang Zhou. Toward general cross-modal signal reconstruction for robotic teleoperation. *IEEE Transactions on Multimedia*, 2023. 1

[6] Bowen Cheng, Ishan Misra, Alexander G Schwing, Alexander Kirillov, and Rohit Girdhar. Masked-attention mask transformer for universal image segmentation. In *Proceedings of the IEEE/CVF conference on computer vision and pattern recognition*, pages 1290–1299, 2022. 7

[7] Meng-Jiun Chiou, Henghui Ding, Hanshu Yan, Changhu Wang, Roger Zimmermann, and Jiashi Feng. Recovering the unbiased scene graphs from the biased ones. In *Proceedings of the 29th ACM International Conference on Multimedia*, pages 1581–1590, 2021. 2

[8] Yuren Cong, Hanno Ackermann, Wentong Liao, Michael Ying Yang, and Bodo Rosenhahn. Nodis: Neural ordinary differential scene understanding. In *European Conference on Computer Vision*, pages 636–653. Springer, 2020. 2

[9] Yuren Cong, Wentong Liao, Hanno Ackermann, Bodo Rosenhahn, and Michael Ying Yang. Spatial-temporal transformer for dynamic scene graph generation. In *Proceedings of the IEEE/CVF international conference on computer vision*, pages 16372–16382, 2021. 2

[10] Kellie Corona, Katie Osterdahl, Roderic Collins, and Anthony Hoogs. Meva: A large-scale multiview, multimodal video dataset for activity detection. In *Proceedings of the IEEE/CVF Winter Conference on Applications of Computer Vision (WACV)*, pages 1060–1068, 2021. 6

[11] Dima Damen, Hazel Doughty, Giovanni Maria Farinella, Sanja Fidler, Antonino Furnari, Evangelos Kazakos, Davide Moltisanti, Jonathan Munro, Toby Perrett, Will Price, and Michael Wray. Scaling egocentric vision: The epic-kitchens dataset. In *European Conference on Computer Vision (ECCV)*, 2018. 5

[12] Ishan Dave, Zacchaeus Scheffer, Akash Kumar, Sarah Shiraz, Yogesh Singh Rawat, and Mubarak Shah. Gabriellav2: Towards better generalization in surveillance videos for action detection. In *Proceedings of the IEEE/CVF Winter Conference on Applications of Computer Vision*, pages 122–132, 2022. 7

[13] Shengyu Feng, Hesham Mostafa, Marcel Nassar, Somdeb Majumdar, and Subarna Tripathi. Exploiting long-term dependencies for generating dynamic scene graphs. In *Proceedings of the IEEE/CVF Winter Conference on Applications of Computer Vision*, pages 5130–5139, 2023. 6

[14] Chen Gao, Jiarui Xu, Yuliang Zou, and Jia-Bin Huang. Drg: Dual relation graph for human-object interaction detection. In *Proc. European Conference on Computer Vision (ECCV)*, 2020. 2

[15] Kristen Grauman, Andrew Westbury, Eugene Byrne, Zachary Chavis, Antonino Furnari, Rohit Girdhar, Jackson Hamburger, Hao Jiang, Miao Liu, Xingyu Liu, et al. Ego4d: Around the world in 3,000 hours of egocentric video. In *Proceedings of the IEEE/CVF Conference on Computer Vision and Pattern Recognition*, pages 18995–19012, 2022. 5

[16] Kaiming He, Xiangyu Zhang, Shaoqing Ren, and Jian Sun. Deep residual learning for image recognition. In *Proceedings of the IEEE conference on computer vision and pattern recognition*, pages 770–778, 2016. 3, 6

[17] Zhi Hou, Baosheng Yu, Yu Qiao, Xiaojiang Peng, and Dacheng Tao. Detecting human-object interaction via fabricated compositional learning. In *Proceedings of the IEEE/CVF Conference on Computer Vision and Pattern Recognition*, pages 14646–14655, 2021. 1

[18] Zhi Hou, Baosheng Yu, and Dacheng Tao. Discovering human-object interaction concepts via self-compositional learning. In *ECCV*, 2022. 1

[19] ASM Iftekhar, Raphael Ruschel, Satish Kumar, Suya You, and BS Manjunath. Dds: Decoupled dynamic scene-graph generation network. In *2025 IEEE/CVF Winter Conference on Applications of Computer Vision (WACV)*, pages 9670–9680. IEEE, 2025. 1, 2, 3, 6

[20] Loshchilov Ilya, Hutter Frank, et al. Decoupled weight decay regularization. *Proceedings of ICLR*, 2019. 6

[21] Jingwei Ji, Ranjay Krishna, Li Fei-Fei, and Juan Carlos Niebles. Action genome: Actions as compositions of spatio-temporal scene graphs. In *Proceedings of the IEEE/CVF Conference on Computer Vision and Pattern Recognition*, pages 10236–10247, 2020. 5

[22] Jingwei Ji, Rishi Desai, and Juan Carlos Niebles. Detecting human-object relationships in videos. In *Proceedings of the IEEE/CVF International Conference on Computer Vision*, pages 8106–8116, 2021. 2

[23] Justin Johnson, Ranjay Krishna, Michael Stark, Li-Jia Li, David Shamma, Michael Bernstein, and Li Fei-Fei. Image retrieval using scene graphs. In *Proceedings of the IEEE conference on computer vision and pattern recognition*, pages 3668–3678, 2015. 2

[24] Siddhesh Khandelwal and Leonid Sigal. Iterative scene graph generation. *Advances in Neural Information Processing Systems*, 35:24295–24308, 2022. 6

[25] Laura Leal-Taixé, Cristian Canton-Ferrer, and Konrad Schindler. Learning by tracking: Siamese cnn for robust target get association. In *Proceedings of the IEEE conference on*

computer vision and pattern recognition workshops, pages 33–40, 2016. 3

[26] Xiangtai Li, Wenwei Zhang, Jiangmiao Pang, Kai Chen, Guangliang Cheng, Yunhai Tong, and Chen Change Loy. Video k-net: A simple, strong, and unified baseline for video segmentation. In *Proceedings of the IEEE/CVF Conference on Computer Vision and Pattern Recognition*, pages 18847–18857, 2022. 1, 7

[27] Yiming Li, Xiaoshan Yang, and Changsheng Xu. Dynamic scene graph generation via anticipatory pre-training. In *Proceedings of the IEEE/CVF Conference on Computer Vision and Pattern Recognition*, pages 13874–13883, 2022. 6

[28] Yong-Lu Li, Siyuan Zhou, Xijie Huang, Liang Xu, Ze Ma, Hao-Shu Fang, Yanfeng Wang, and Cewu Lu. Transferable interactiveness knowledge for human-object interaction detection. In *Proceedings of the IEEE Conference on Computer Vision and Pattern Recognition*, pages 3585–3594, 2019. 2

[29] Tsung-Yi Lin, Michael Maire, Serge Belongie, James Hays, Pietro Perona, Deva Ramanan, Piotr Dollár, and C Lawrence Zitnick. Microsoft coco: Common objects in context. In *European conference on computer vision*, pages 740–755. Springer, 2014. 6

[30] Xin Lin, Chong Shi, Yibing Zhan, Zuopeng Yang, Yaqi Wu, and Dacheng Tao. Td2-net: Toward denoising and debiasing for dynamic scene graph generation. *ArXiv*, abs/2401.12479, 2024. 2, 6

[31] Xiaochen Liu, Pradipta Ghosh, Oytun Ulutan, B. S. Manjunath, Kevin Chan, and Ramesh Govindan. Caesar: cross-camera complex activity recognition. In *Proceedings of the 17th Conference on Embedded Networked Sensor Systems*, page 232–244, New York, NY, USA, 2019. Association for Computing Machinery. 1

[32] Yang Liu, Qingchao Chen, and Andrew Zisserman. Amplifying key cues for human-object-interaction detection. In *European Conference on Computer Vision*, pages 248–265. Springer, 2020. 2

[33] Jiale Lu, Lianggangxu Chen, Youqi Song, Shaohui Lin, Changbo Wang, and Gaoqi He. Prior knowledge-driven dynamic scene graph generation with causal inference. In *Proceedings of the 31st ACM International Conference on Multimedia*, page 4877–4885, New York, NY, USA, 2023. Association for Computing Machinery. 2, 6

[34] Yichao Lu, Himanshu Rai, Jason Chang, Boris Knyazev, Guangwei Yu, Shashank Shekhar, Graham W Taylor, and Maksims Volkovs. Context-aware scene graph generation with seq2seq transformers. In *Proceedings of the IEEE/CVF International Conference on Computer Vision*, pages 15931–15941, 2021. 2

[35] Tim Meinhardt, Alexander Kirillov, Laura Leal-Taixe, and Christoph Feichtenhofer. Trackformer: Multi-object tracking with transformers. In *Proceedings of the IEEE/CVF conference on computer vision and pattern recognition*, pages 8844–8854, 2022. 3

[36] Sayak Nag, Kyle Min, Subarna Tripathi, and Amit K. Roy-Chowdhury. Unbiased scene graph generation in videos. In *2023 IEEE/CVF Conference on Computer Vision and Pattern Recognition (CVPR)*, pages 22803–22813, 2023. 1, 2, 6

[37] Thong Thanh Nguyen, Xiaobao Wu, Yi Bin, Cong-Duy T Nguyen, See-Kiong Ng, and Anh Tuan Luu. Motion-aware contrastive learning for temporal panoptic scene graph generation. In *Proceedings of the AAAI Conference on Artificial Intelligence*, pages 6218–6226, 2025. 7

[38] Jing Qi, Li Ma, Zhenchao Cui, and Yushu Yu. Computer vision-based hand gesture recognition for human-robot interaction: a review. *Complex & Intelligent Systems*, 10(1):1581–1606, 2024. 1

[39] Raphael Ruschel, A. S. M. Iftekhar, B. S. Manjunath, and Suya You. Bload: Enhancing neural network training with efficient sequential data handling. *arXiv preprint arXiv:2310.10879*, 2023. 6

[40] Samuel Schulter, Paul Vernaza, Wongun Choi, and Manmohan Chandraker. Deep network flow for multi-object tracking. In *Proceedings of the IEEE Conference on Computer Vision and Pattern Recognition*, pages 6951–6960, 2017. 3

[41] Xindi Shang, Donglin Di, Junbin Xiao, Yu Cao, Xun Yang, and Tat-Seng Chua. Annotating objects and relations in user-generated videos. In *Proceedings of the 2019 on International Conference on Multimedia Retrieval*, pages 279–287. ACM, 2019. 5

[42] Karthikeyan Shanmuga Vadivel, Thuyen Ngo, Miguel Eckstein, and BS Manjunath. Eye tracking assisted extraction of attentionally important objects from videos. In *Proceedings of the IEEE Conference on Computer Vision and Pattern Recognition*, pages 3241–3250, 2015. 4

[43] Jing Shi, Yiwu Zhong, Ning Xu, Yin Li, and Chenliang Xu. A simple baseline for weakly-supervised scene graph generation. In *Proceedings of the IEEE/CVF International Conference on Computer Vision*, pages 16393–16402, 2021. 2

[44] Gunnar A Sigurdsson, GÜl Varol, Xiaolong Wang, Ali Farhadi, Ivan Laptev, and Abhinav Gupta. Hollywood in homes: Crowdsourcing data collection for activity understanding. In *European Conference on Computer Vision*, pages 510–526. Springer, 2016. 5

[45] Peize Sun, Jinkun Cao, Yi Jiang, Rufeng Zhang, Enze Xie, Zehuan Yuan, Changhu Wang, and Ping Luo. Trantrack: Multiple object tracking with transformer. *arXiv preprint arXiv:2012.15460*, 2020. 3

[46] Kaihua Tang, Hanwang Zhang, Baoyuan Wu, Wenhan Luo, and Wei Liu. Learning to compose dynamic tree structures for visual contexts. In *Proceedings of the IEEE/CVF conference on computer vision and pattern recognition*, pages 6619–6628, 2019. 2

[47] Yao Teng, Limin Wang, Zhifeng Li, and Gangshan Wu. Target adaptive context aggregation for video scene graph generation. In *Proceedings of the IEEE/CVF International Conference on Computer Vision*, pages 13688–13697, 2021. 2

[48] Oytun Ulutan, ASM Iftekhar, and Bangalore S Manjunath. Vsgnet: Spatial attention network for detecting human object interactions using graph convolutions. In *Proceedings of the IEEE/CVF Conference on Computer Vision and Pattern Recognition*, pages 13617–13626, 2020. 2

[49] Bo Wan, Desen Zhou, Yongfei Liu, Rongjie Li, and Xuming He. Pose-aware multi-level feature network for human object interaction detection. In *Proceedings of the IEEE International Conference on Computer Vision*, pages 10210–10219, 2023. 2

national Conference on Computer Vision, pages 9469–9478, 2019. 2

[50] Guan Wang, Zhimin Li, Qingchao Chen, and Yang Liu. Oed: Towards one-stage end-to-end dynamic scene graph generation. In *Proceedings of the IEEE/CVF Conference on Computer Vision and Pattern Recognition*, pages 27938–27947, 2024. 6

[51] Suchen Wang, Yueqi Duan, Henghui Ding, Yap-Peng Tan, Kim-Hui Yap, and Junsong Yuan. Learning transferable human-object interaction detector with natural language supervision. In *Proceedings of the IEEE/CVF Conference on Computer Vision and Pattern Recognition*, pages 939–948, 2022. 1

[52] Shuang Wang, Lianli Gao, Xinyu Lyu, Yuyu Guo, Pengpeng Zeng, and Jingkuan Song. Dynamic scene graph generation via temporal prior inference. In *Proceedings of the 30th ACM International Conference on Multimedia*, page 5793–5801, New York, NY, USA, 2022. Association for Computing Machinery. 6

[53] Tiancai Wang, Rao Muhammad Anwer, Muhammad Haris Khan, Fahad Shahbaz Khan, Yanwei Pang, Ling Shao, and Jorma Laaksonen. Deep contextual attention for human-object interaction detection. In *Proceedings of the IEEE International Conference on Computer Vision*, pages 5694–5702, 2019. 2

[54] Wenbin Wang, Ruiping Wang, Shiguang Shan, and Xilin Chen. Exploring context and visual pattern of relationship for scene graph generation. In *Proceedings of the IEEE/CVF Conference on Computer Vision and Pattern Recognition*, pages 8188–8197, 2019. 2

[55] Wenbin Wang, Ruiping Wang, and Xilin Chen. Topic scene graph generation by attention distillation from caption. In *Proceedings of the IEEE/CVF International Conference on Computer Vision*, pages 15900–15910, 2021. 2

[56] Zhongdao Wang, Hengshuang Zhao, Ya-Li Li, Shengjin Wang, Philip Torr, and Luca Bertinetto. Do different tracking tasks require different appearance models? *Advances in Neural Information Processing Systems*, 34:726–738, 2021. 7

[57] G Welch. An introduction to the kalman filter. 1995. 3

[58] Nicolai Wojke, Alex Bewley, and Dietrich Paulus. Simple online and realtime tracking with a deep association metric. In *2017 IEEE international conference on image processing (ICIP)*, pages 3645–3649. IEEE, 2017. 3

[59] Jingkang Yang, Wenzuan Peng, Xiangtai Li, Zujin Guo, Liangyu Chen, Bo Li, Zheng Ma, Kaiyang Zhou, Wayne Zhang, Chen Change Loy, and Ziwei Liu. Panoptic video scene graph generation. In *CVPR*, 2023. 1, 2, 5, 7

[60] Fangao Zeng, Bin Dong, Yuang Zhang, Tiancai Wang, Xiangyu Zhang, and Yichen Wei. Motr: End-to-end multiple-object tracking with transformer. In *European Conference on Computer Vision*, pages 659–675. Springer, 2022. 3

[61] Ji Zhang, Kevin J Shih, Ahmed Elgammal, Andrew Tao, and Bryan Catanzaro. Graphical contrastive losses for scene graph parsing. In *Proceedings of the IEEE/CVF Conference on Computer Vision and Pattern Recognition*, pages 11535–11543, 2019. 2

[62] Yong Zhang, Yingwei Pan, Ting Yao, Rui Huang, Tao Mei, and Chang-Wen Chen. End-to-end video scene graph generation with temporal propagation transformer. *IEEE Transactions on Multimedia*, 26:1613–1625, 2023. 6

[63] Huiyu Zhou, Yuan Yuan, and Chunmei Shi. Object tracking using sift features and mean shift. *Computer vision and image understanding*, 113(3):345–352, 2009. 3

[64] Xizhou Zhu, Weijie Su, Lewei Lu, Bin Li, Xiaogang Wang, and Jifeng Dai. Deformable detr: Deformable transformers for end-to-end object detection. *arXiv preprint arXiv:2010.04159*, 2020. 3